Available online at sjuoz.uoz.edu.krd

Science Journal of University of Zakho
Vol. 11, No. 1, pp. 112– 118, January-March 2023

journals.uoz.edu.krd

p-ISSN: 2663-628X
e-ISSN: 2663-6298

INVESTIGATING THE IMPACT OF GROWTH TEMPERATURES ON THE ZNO NANORODS PROPERTIES GROWN WITH SIMPLEST SPRAY TECHNIQUE

Mohammed Kadhim Jaqsi [a,*], Awaz Adil Kareem [a], Ahmed Fattah Abdullrahman [a,b]

[a] Department of Physics, Faculty of Science, University of Zakho, Kurdistan Region-Iraq (mohammed.jaqsi; awaz.kareem; ahmed.abdulrahman @uoz.edu.krd)
[b] Department of Computer and Communications Engineering, College of Engineering, Nawroz University, Kurdistan Region, Iraq (ahmed.abdulrahman@uoz.edu.krd)

Received: *23 Nov., 2022 /* ***Accepted:*** *19 Dec., 2023 /* ***Published:*** *20 Feb., 2023* ***https://doi.org/10.25271/sjuoz.2022.11.1.1072***

ABSTRACT:
The simplest chemical spray approach has been used to grow the zinc oxide (ZnO) nanorods (NRs). For spraying, a basic perfume automizer was employed. Additionally, utilizing a variety of characterization techniques, the effects of various growth temperatures on the ZnO NRs properties were looked into and evaluated. The results of the investigation demonstrated that the growing temperature significantly affects all-characteristics properties of the ZnO NRs fabricated using the most straightforward spray approach. At various growth temperatures, the average diameters (size) and average crystalline sizes along with (002) of grown ZnO NRs were in the ranges of (47.89-51.29) nm and (44.128-52.565) nm, respectively. The hexagonal wurtzite plane was the optimum direction for ZnO NRs to be oriented, and as growth temperatures are raised. The absorption edge changed toward longer wavelengths and as growth temperature increased, the average absorbance also increased. The optical analysis reveals that the direct Eg. of the produced ZnO NRs lies in the (3.182-3.250) eV range.

KEYWORDS: Simplest Spray Method, ZnO, Nanorods, Growth Temperature, Surface Morphology

1. INTRODUCTION

Given its distinctive qualities, which include its broad direct band gap (3.37 eV), visibility in the visual range, availability in nature, no poisoning, strong electrochemical stabilization, and maneuverability over resistivity overhead the domain of (10^{-3}-10^{5}) Ocm [1]. In recent years, ZnO has emerged as a versatile and essential n-type semiconducting compound. Additionally, ZnO has great optical and electrical properties, a wide exciton binding energy of (60 meV) at RT, and is biocompatible. It also has high mechanical, chemical, and thermal stability [2]. These characteristics make the ZnO suitable for optoelectronic components like gas sensors, light emitting components, dye-sensitive solar cells, photocatalysts, transparent conducting layers, blocking layers in flexible organic solar cells, and thin film transistors [3]. ZnO is currently the subject of extensive investigation by several groups. This benefit is due to a variety of factors, such as the enormous area of the promising implementation where it was predicted that the zinc oxide will carry out preferable compared other semiconductors types, the approachability of the ZnO perspicuous materials with a variety of individual properties, inexpensive, and high levels of clarity [4]. Due to promises of enhanced implementations achievement, device downsizing, depress exhaustion power, and the materials with remarkable attributes, the nanotechnology sector has increased in prominence alongside ZnO's expanding benefits as a semiconductor [5]. The II-VI semiconductor materials group of inorganic binary compounds includes ZnO [6].
Due to the individual and fascinating optical, mechanical, electrical, thermo-electrical, and chemical properties of ZnO numerous nanostructures materials as well as their potential technological applications have attracted significant interest, particularly in electronics, optics, and the enormous variety of photonic usages [7,8]. Scientists in the domain of semiconductor nanotechnology have recently become very interested in one-dimensional (1D) semiconductor nanostructures like nanorods, nanotubes, nanobelts, and nanowires due to their distinguishing properties and the promising for using them as building blocks for future electronic and photonic devices or applications like UV photodetector, UV nano-laser, solar cell, light emitting diode (LED), gas sensor, and field emittance microscopes. It is widely acknowledged that one-dimensional nanostructures of various types are useful materials for getting the influence of mechanical properties or thermal and electrical convey on the dimensionality and stenography in size [9].
The successive ionic layer adsorption reaction (SILAR), chemical bath deposition, modified chemical-bath deposition, sol-gel, electrodeposition, sonochemical method, spray pyrolysis, chemical vapor deposition, hydrothermal synthesis, and sol-gel are some of the physical and chemical processes that can be used to make these ZnO NRs [10-12]. The simplest spray pyolysis technique is the most efficient, high-performing, and effective growth method for growing various nanomaterials and nanostructures due to its advantages, including the formation of high-density arrays, high crystal quality, and large capacity of growth vessel used, low cost, simplicity, and reproducibility; the need for a complex growth system; and environmental considerations [13, 14]. Also, with MCBD method, one can be growing numerous nanostructures, on the numerous substrates (flexible, nonflexible, organic and inorganic), where it does not require the conductive substrates [14].
Using the simplest spray pyrolysis techniques, numerous growth parameters such as; growth temperature, precursor concentration, growth temperature, post-annealing conditions, type of substrates, and growth solution pH, have numerous

* Corresponding author

effects on the synthesis and quality of ZnO nanostructures [15, 16]. The simplest spray pyrolysis approach was used in this study to create ZnO nanorods utilizing perfume atomizers. We, therefore, looked into how varied substrate growth temperatures ranging from 200 to 400 oC, affected the characteristics of ZnO nanorods.

2. EXPERIMENTAL METHODS

Without further purification, Sigma-Aldrich (SA) was employed to get all of the chemical components for this study, including zinc chloride (ZnCl2) and aqueous ammonia solution (NH4OH) with a palliated ratio of (25 percent). The simplest spray technique deposition was performed using perfume atomizers. The simplest spray approach along with several growth processes was used to produce the ZnO NRs across the microscopic glass slide. The first step was to cut and clean the microscopic glass slide substrates in the ultrasonic bath for 20 minutes each using pure ethanol (96%), acetone, and double-distilled water. The tiny glass substrate was then cured at ambient temperature [17]. The second step was to create ZnO NRs with various growth temperatures, the simplest chemical spray pyrolysis approach was used in conjunction with inexpensive perfume atomizers. 0.1 M of ZnCl2 was dissolved in double-distilled water using a magnetic stirrer under continuous stirring to produce a uniformly transparent growth solution and fully dissolved ZnCl2 solution.

The resulting zinc solution's pH was then changed to 8.5 using a 25% water solution of NH4OH ammonia. Drop by drop, under magnetic stirring, NH4OH was added to the growth zinc solution that had been created. After adjusting the pH of the zinc solution to pH 8.5, the color of the growth zinc solution changed from transparent to milky thick white. Simple scent automizers that had been thoroughly cleansed were filled with the ready-made milky dense white growth zinc solution for making ZnO NRs [12]. At varied growth temperatures, which are 200 oC, 300 oC, and 400 oC, the generated milky growth zinc solution was sprayed over the entire cleaned glass substrates. The photograph of the simplest spray method system is shown in the Fig.1

The prepared ZnO NRs samples were given the matching labels of a, b, and c. The following conditions have been met while using the simplest chemical spray approach. The precursor growth zinc solution flow rate is around 1 mL/sec, and the distance between the glass substrates and the perfume atomizer was about 35 cm. The duration of each chemical spray growth cycle is 2 seconds, followed by a 15-second pause. Prior to beginning the subsequent growth chemical spray cycle, the waiting period allows the glass substrate to reach the necessary temperature for growth. Three cycles of this straightforward chemical spray growth procedure were required to obtain uniform zinc oxide nanorods over the entire microscopic glass substrates at various growth temperatures. After completing the chemical spraying growth procedure, the ZnO NRs sample that was produced at various growth temperatures was gradually cooled down to room temperature. The fabricated ZnO nanorods were annealed in the air using a tube furnace at 550 oC for 1 hour in order to reduce the atomic mismatch of the ZnO NRs sample and improve the structural and optical properties of the ZnO nanorods.

Finally, the samples of ZnO nanorods that were made at numerous temperatures have been examined and characterized utilizing a variety of characterization techniques. A FESEM system of type (FEI-Nova Nano SEM-450), an elevated XRD system with a scanning angle of 2theta (20-80), and a Raman system, were used to examine the morphology and surface properties of prepared ZnO nanorods with numerous growth temperatures. These properties included size, shape, direction, and chemical properties, as well as structural (XRD patterns, defects, and crystalline size), optical, and phonon vibrational study or Raman spectra.

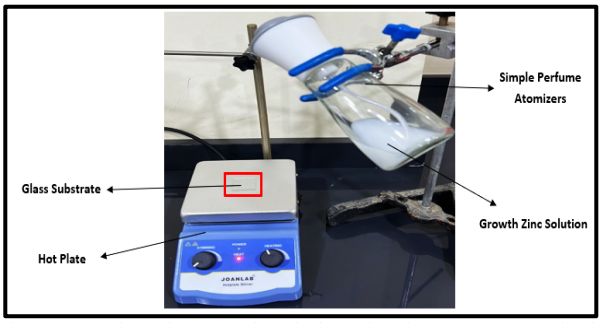

Figure 1. The Photograph of the Simplest Spray Method System

3. 3. RESULTS AND DISCUSSION

The FESEM images of the ZnO nanorods produced using the simplest chemical spray approach at various growth temperatures are shown in Figure 2. From Figure 1, it is clear that the ZnO nanorods were successfully formed over the entire glass substrates by utilizing a straightforward scent automizer. Additionally, the shape (formation), density distribution, average size (diameter), orientation, and alignment of ZnO NRs are significantly impacted by changes in growth temperatures.

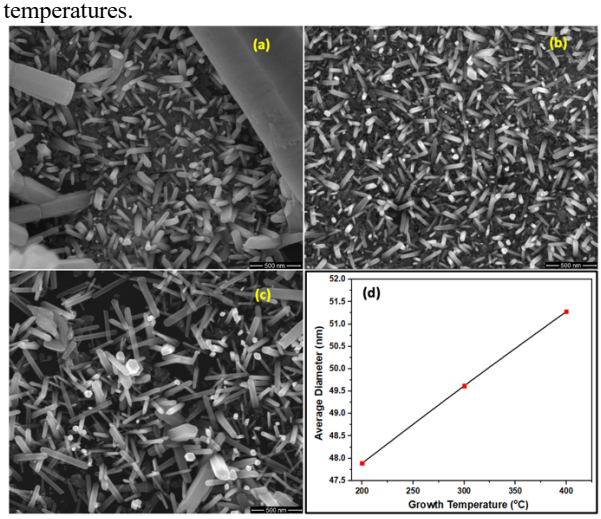

Figure 2. The FESEM Images Analysis of ZnO Nanorods Fabricated Using the Easiest Chemical Spray Technique with distinct Growth Temperatures: (a) 200 oC, (b) 300 oC, and (c) 400 oC. The average ZnO nanorod diameter is plotted against the growth temperature in Figure 1(d).

Obviously, at low growth or growth temperature 200 oC as displayed in Figure 2 (a), low density, short length, non-uniform shape, incompletely, non-homogenous ZnO NRs were produced with oriented randomly with average diameter of 47.89 nm over the whole glass substrates. However, with increasing the growth temperature to 300 oC, the remarkable change in morphological characteristics regarding shape, density distribution, size, alignment, and orientation of ZnO NRs were identified as exhibited in Figure 2 (b). The average diameter of ZnO NRs synthesized at 300 C is about 49.62 nm. In addition, Figure 2 (c) shows that the alignment, shape, size, orientation, density distribution, and homogeneity of ZnO NRs have been significantly improved with increases the growth temperature to 400 oC. Also, the most of obtained ZnO NRs were grown and oriented along c-axis or vertically aligned with average diameter is about 51.28 nm.

The morphological properties such as shape, size, density, homogeneity and orientation of the ZnO NRs were improved with increasing the growth temperatures

may be due to the enhancement of the kinetics of the growth supporting the quick precipitation of ZnO add-atoms, resulting in a larger size of ZnO NRs. This indicates that increasing the temperature would improve the aggregation and accelerate the reactive nucleation add-atoms during the solvothermal synthesis [17].

Figure 3 depicts the corresponding EDX analysis of the elemental chemical composition of ZnO NRs made utilizing the most straightforward chemical spray approach at various growth temperatures. One can see that the ratio of zinc (Zn) to oxygen (O2) is significantly impacted by the growth temperature in the range of (200-400) oC. According to EDX limitations, the matching EDX analysis of Figure 3 shows the (Zn) and (O), which correspond to the typical texture of ZnO, without the occurrence of every pollutant or substrate indicative (signal). For all samples of ZnO nanorods that were tested and made using various temperatures for chemical spray growing, the ratio of Zn to O was nearly the same. At various growth temperatures, the produced NRs are confirmed to be pure ZnO by the molecular ratio of Zn:O, which is almost 1:1 as derived from quantitative EDX analysis data.

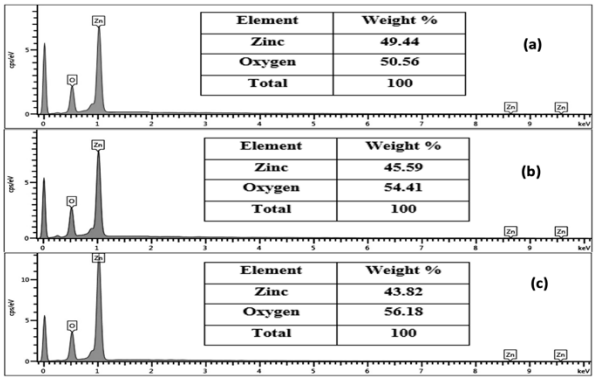

Figure 3. The Representative EDS Analysis of ZnO Nanorods Fabricated with Simplest Chemical Spray Technique at Numerous Growth Temperatures: (a) 200 oC, (b) 300 oC, and (c) 400 oC.

Figure 4 illustrates the X-ray diffraction (XRD) patterns of synthetic ZnO nanorods made utilizing the simplest chemical spray approach at various growth temperatures. The conclusion was made that the zinc oxide wurtzite hexagonal phase structure adhered to the standard database spectrum because of all detected diffraction peaks in all three XRD patterns (JCPDS card-No. 01-080-0075). There are no peaks of diffraction that belong to the impurities that were seen, demonstrating that ZnO NRs were fabricated at various growth temperatures using a straightforward chemical spray technique. Additionally, it should be noted that all ZnO NRs samples produced showed preferential growth along the plane's c-axis at the 2 = 34.420, 34.425, and 34.435 degrees Celsius, respectively, for 200 oC, 300 oC, and 400 oC. The ZnO nanorods resort to develop in the (002) orientation due to it has the lowest free surface energy density in the ZnO crystal [18].

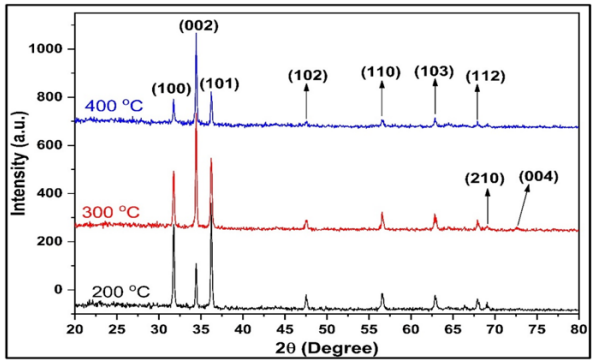

Figure 4. The XRD Patterns of ZnO Nanorods Fabricated with Simplest Chemical Spray Technique at Numerous Growth Temperatures.

Figure 4(a) shows that when ZnO NRs were grown at 200 °C, the (101) diffraction peak was somewhat more prominent than the (002) and (101) and almost equal to the value of (101). This proved that the majority of ZnO nanorods are not developed vertically or in a uniform orientation, but rather are almost more inclined to grow in the (100) and (101) planes than the (002) plane. The powerful diffraction peaks along the (002) plane with very weak diffraction peaks from other planes or surfaces are observed at 2 values of 34.425 and 34.435 of ZnO NRs, however, when the growth temperature of ZnO NRs is increased from 300 °C to 400 °C, as shown in Figure 4 (b and c). This indicated that when the growth temperature rose, the alignment improved and increased, and the majority of vertically aligned ZnO nanorods grew on the entire glass substrate [19].

Additionally, the XRD scans demonstrated that the nanorods grew vertically on top of used substrates, particularly all along c-axis of the wurtzite hexagonal structure. This peak, designated (002), is strong and distinct [20]. The results XRD patterns under examination exhibit good agreement with the findings of the FESEM and previous studied [21-24]. The majority of the samples that were tested showed diffraction peaks from surfaces with the numbers (101), (103), (102), (112), (110), and (100), and that indicated a sizable number of ZnO nanorods were orientated in numerous orientations. Figure 4 shows that as the growth temperature is raised in the range of (200-400) °C, the intensity of the ZnO NRs (002) peak gradually increases. The ZnO nanorod arrays are positioned getting up (perpendicular) to the surface of the glass substrate and in the c-axis direction, according to the higher intensity of the diffraction peaks (002) [17]. Additionally, the plane in ZnO nanorod samples is well-aligned as the growth temperature rises, enabling the ZnO samples to detect more X-rays. The peak intensity rises with the growing temperature for this reason. It is worthwhile to point out that as growth temperature rises, the diffraction peaks (002) get higher and smaller, proving that ZnO's crystalline quality improves.

Table 1. The impact of numerous growth temperatures on the ZnO nanorods produced utilizing a straightforward chemical spray method's average crystalline size, hexagonal cell volume, dislocation density, and bond length.

Growth Temperature (°C)	Plane	Crystalline Size (nm)	Volume (Å^3)	δ ×10^{-6} (Å^{-2})	Bond Length (Å)
200	**100**	42.125	51.454	5.635	2.032
300	**100**	40.908	51.691	5.975	2.035
400	**100**	33.320	51.454	9.007	2.032
200	**002**	44.218	40.753	5.114	1.883
300	**002**	48.352	40.735	4.277	1.880
400	**002**	52.565	40.701	3.619	1.879
200	**101**	48.283	35.131	4.290	1.789
300	**101**	37.754	35.131	7.020	1.789
400	**101**	37.071	35.131	7.280	1.789

Using the Debye-Scherer formula, the average crystalline size of ZnO NRs along the three prominent peak diffractions (100), (002) and (101) planes are assessed at various growth temperatures. The results are shown in Table 1 [25]

$$D = \frac{k\lambda}{\beta cos\theta} \qquad (1)$$

where k is a constant, assumed to be 0.9, where is the X-ray source's wavelength, β is the full width at half maximum (FWHM) in radians, and θ is the Bragg diffraction angle.

As growth temperature rises, the crystal size of the produced ZnO NRs along (002) plane decreases. The following equation determines the dislocation density along the three prominent peak diffractions (100), (002), and (101) planes, This indicates the quantity of flaws in the [25].

$$\delta = \frac{1}{D^2} \qquad (2)$$

where D is crystallite size.

Table 1 shows the results of an investigation into how numerous growth temperatures affected the volume of hexagonal cells and bond length of ZnO NRs. Using the formula given, the ZnO bond length is calculated [26].

$$L = \sqrt{\frac{a^2}{3} + \left(\frac{1}{2} - u\right)^2 c^2} \qquad (3)$$

The positional parameter u, which is connected to the c/a ratio and determines how far apart each atom is from the next along the 'c' axis in the wurtzite hexagonal structure, is given by [26]:

$$u = \frac{a^2}{3c^2} + 0.25 \qquad (4)$$

The following equation was used to get the hexagonal cell's volume (V) [26]:

$$V = \frac{\sqrt{3}}{2} a^2 c \qquad (5)$$

where a and c are the lattice constants.

Table 2. The impact of varying growth temperature on the structural characteristics and lattice parameters of ZnO nanorods made utilizing a straightforward chemical spray method.

Growth Temperature (ºC)	Plane	FWHM	2θ	c (Å)	ℇc%	a (Å)	ℇa%	Interplanar Distance (Å)
200	**100**	0.196079	31.775	5.628	8.023	3.249	-0.145	2.814
300	**100**	0.201887	31.725	5.636	8.189	3.254	0.009	2.818
400	**100**	0.247896	31.775	5.628	7.913	3.249	-0.132	2.814
200	**002**	0.188083	34.420	5.207	-0.055	3.006	-7.612	2.604
300	**002**	0.172004	34.425	5.206	-0.069	3.006	-7.625	2.603
400	**002**	0.158222	34.435	5.205	-0.198	3.005	-7.639	2.602
200	**101**	0.173111	36.225	4.956	-4.88	2.861	-12.072	2.478
300	**101**	0.221392	36.225	4.956	-4.88	2.861	-12.072	2.478
400	**101**	0.225472	36.225	4.956	-4.977	2.861	-12.0612	2.478

Table 2 provides information on the structural characteristics, peak position, intensity, lattice constants, and internal stresses (ℇc) and (ℇa) of the ZnO hexagonal structure along the three prominent peak diffractions (100), (002), and (101) planes for various growth temperatures. Bragg's law is used to determine the lattice constants (a & c) of the hexagonal ZnO wurtzite structure along (002) peak [27]:

$$a = \sqrt{\frac{1}{3}} \frac{\lambda}{\sin\theta} \qquad (6)$$

$$c = \frac{\lambda}{\sin\theta} \qquad (7)$$

where (θ) and (λ) were the diffraction peak angle, and the X-ray source wavelength respectively.

The strains and stress (ℇc) and (ℇa) are obtained from the following formulae for the deposited ZnO NRs along the c-axis and a-axis, respectively [27]:

$$\varepsilon_a = \left(\frac{a - a_o}{a_o}\right) \times 100\% \qquad (8)$$

$$\varepsilon_c = \left(\frac{c - c_o}{c_o}\right) \times 100\% \qquad (9)$$

where ao and co the common lattice constants for unstrained ZnO NRs found in the shared database are given.

It's noteworthy to notice that the strains (ℇc) and (ℇa) along the three prominent peaks are dramatically altered as the growth temperatures changed, as illustrated in Table 2. The existence of variance in the values of strains (ℇh) and (ℇa) is caused by variations in the interplanar spacing measurements, most occurs as a consequence of stacking fault and lattice mismatch flaws between crystal growth and substrate. A negative strain magnitude is linked to the compressed strain and denotes a contraction of the lattice, whereas a positive strain magnitude is linked to the tensile strain and pointed an increase in the lattice constant. According to Bragg's law, the plane spacing of wurtzite of ZnO NRs is determined for various growth temperatures and is shown in Table 2 [17]:

$$\frac{1}{d^2} = \frac{4}{3}\left(\frac{h^2 + hk + k^2}{a^2}\right) + \frac{l^2}{c^2} \qquad (10)$$

where a and c are the lattice constants defined.

To demonstrate how changing growth temperatures affect the optical features of ZnO nanorods, RT uses ultraviolet (UV) visible spectroscopy to examine the optical qualities based on the absorption spectra. Figure 5 shows how numerous growth temperatures affect the optical absorption spectra of ZnO nanorods in the 300–800 nm wavelength range. The UV area at wavelengths below 400 nm exhibits significant absorbance (low transparency) and the visible region exhibits low absorbance (high transparency), which are ZnO properties. All ZnO NRs samples have a pronounced UV absorption edge that is discovered at a wavelength of about 380 nm [22, 23], which matched to the optical Eg of the ZnO nanorods.

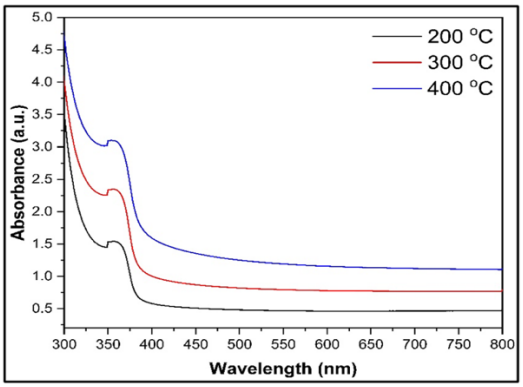

Figure 5. The Optical Absorption Spectrums of ZnO Nanorods Fabricated with Simplest Chemical Spray Technique at Numerous Growth Temperatures.

The absorption edge changed toward longer wavelength as growth temperature increased from 200 oC to 400 oC. Reduced Eg, the transitional gap between energy levels, caused the absorption edge to move to higher wavelengths [18]. It was found that the average absorbance increases when the growth temperature rises from 200 oC to 400 oC, as illustrated in Figure 5. After the growth temperature was raised from 200 oC to 400 oC, there may have been an increase in hydroxide accumulation at grain boundaries and topographical changes to the ZnO nanorods. Further, the increase in the absorption spectrum that occurs when the growth temperature rises from 200 oC to 400 oC may be caused by the larger crystalline size that causes a greater absorption of light. Low absorption values at long wavelengths were leaded to by pollutions in the ZnO NRs layer, such as oxygen vacancies and donor-impurity-serving interstitial Zn atoms [22, 18]. In addition, ZnO nanorod absorbance at 400 oC at other production temperatures showed that the other samples had good crystallinity. Moreover, have a large interior surface area for the adsorption of electrolytes. From the obtained optical results, one can conclude that the fabricated ZnO nanorods samples from simplest spray method with different growth temperatures can be used for different application such as UV sensor, gas sensor, solar cell, and pH sensor.

Figure 6 illustrates an extrapolation of the linear portion of (αhν)2 versus h to produce a Tauc formula regularly to determine the optical Eg of ZnO NRs using absorption spectra. The below formulae enabling employed to compute the Eg of ZnO NRs developed at numerous growth temperatures ranging (200-400) oC is illustrated in the Figure 5 [19]:

$$(\alpha h\nu)^2 = A(h\nu - E_g)^n \qquad (11)$$

Where hν, A, Eg, and α is photon energy, constant, coefficient of absorption spectra, and the optical band-gap, and n is factor depended on the form or types of the transmission which is equal to 0.5 for direct band gap. Also, the (α) coefficient for the transmittance spectrum is calculated by utilizing below formula [25]:

$$\alpha = \frac{\ln(\frac{1}{T})}{d} \qquad (12)$$

where d, and T is the ZnO NRs nanofilms thickness, and transmittance rate of ZnO nanofilm.

The optical Eg of the ZnO semiconductor, which is indicated by the transition area that agreement to the direct transition between the borders of the valance and conduction bands, was found to be approximately 3.20 eV from the plots. At numerous growth temperatures, the predicted direct optical Eg of ZnO NRs was (3.250, 3.233, and 3.182) eV for 200 oC, 300 oC, and 400 oC, respectively.

It is possible to assume that the observed variance of the Eg with numerous growth temperatures is associated to the crystalline quality (FWHM) of growth ZnO, such as agglomeration of the nanorods which increases the number of dislocations and defects, strains, random orientation of the nanorods [19, 25]. The acquired Eg values of several ZnO NRs produced at various growth temperatures using the simplest chemical spray approach are almost in perfect accord with these earlier research [22]. The obtained Eg of ZnO NR produced at numerous growth temperatures is around 3.37 eV lower than that of ZnO bulk. This is because the creation of ZnO NRs has an optical confinement effect [22].

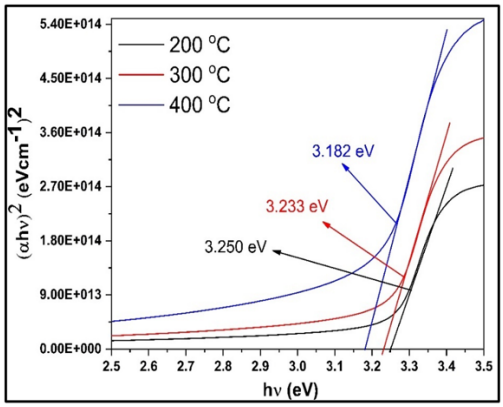

Figure 6. The Tauc Plot (αhν)2 against Eg of ZnO Nanorods Formed with the Easiest Chemical Spray Technique at Numerous Growth Temperatures

The sample does not need to be specially prepared for measurements, because the one of the non-destructive and contactless research methods is micro-Raman scattering. It also works well for analyzing the phase orientation, material quality, phonon interaction, and transport parameters [28]. As a member of the space group C_{6v}^4, Wurtzite ZnO is predicted to exhibit all eight sets of phonon modes at wave vector k ≈ 0 (Γ point). Six of ZnO's eight phonon modes are optical phonon modes, and the remaining two are acoustic. Group theory states that the optical mode at the Brillouin zone's point can be represented by [29].

$$\Gamma = 1A_1 + 2B_1 + 1E_1 + 2E_2 \qquad (13)$$

Among these are the Raman active modes like (1A1, 1E1, and 2E2). While the (A1 and E1) modes are infrared actives modes, only the E2 mode is Raman Active. The 2B1 modes are silent modes. The (A1, E1) modes are isolated from the longitudinal optical (LO) and transverse optical (TO) phonons. The two frequencies of the E2 symmetric non-polar phonon modes are E2(high) and E2(low), which are connected to O2 atoms and the Zn sub-lattice, respectively. Raman scattering is only active in the E2(high) and A1 LO of ZnO NRs because it is perpendicular to their c-axis [30, 31].

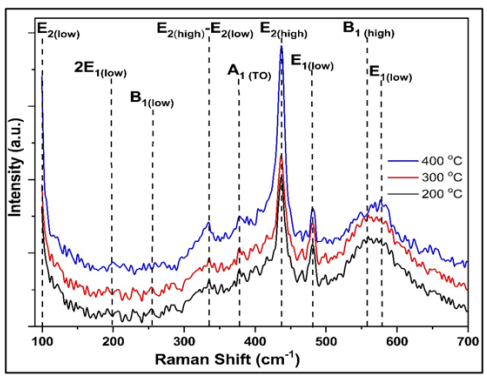

Figure 7. ZnO Nanorods Fabricated with the Easiest Chemical Spray Technique and Analyzed by Raman Spectroscopy at Various Growth Temperatures.

In the current study, it is examined how numerous growth temperatures affect the Raman spectroscopy of ZnO NRs that have been formed utilizing the most basic chemical spray approach. The typical Raman spectra of ZnO NRs made on glass substrates at various growth temperatures are displayed in Figure 7. For the ZnO NRs formed at all growth temperatures, there are prominent and distinct peaks that arise at about 100 cm-1 and 436 cm-1, respectively. These peaks correlate to the inherent properties of the Raman active E2(low) and E2(high) modes of the hexagonal wurtzite ZnO. The fact that the produced ZnO nanorods exhibit a strong and prominent peak of the E2(High) mode without the E2(Low) mode indicates that they possess a high-quality hexagonal wurtzite structure [32].

For the ZnO nanorods produced in all samples, the faint peaks at around 331 cm-1, which are connected to the E2(high) - E2(low) (multiple phonon process), and the A1 (TO) mode are visible [37, 42]. Peaks at 481 cm-1, 563 cm-1, and 582 cm-1 correspond to contaminants and structural flaws in the E1(Low) mode (oxygen vacancies and Zn interstitials). The ZnO NRs Raman active peak intensities increased at 400 oC are higher than those of ZnO nanorods formed at other growth temperatures, indicating an improvement in the nanorods' crystal quality and/or an expansion of the nanorod arrays' coverage of the substrate [33].

4. CONCLUSION

The simplest chemical spray approach was effectively used to fabricate an array of vertically semi-aligned ZnO NRs at various growth temperatures. The morphological, structural, phonon vibration study, and optical characteristics of fabricated ZnO NRs are significantly impacted by the investigations of various growth temperatures. Additionally, it was determined through obtained properties that the best growth temperature for ZnO NRs using the simplest spray approach is 400 °C. The average diameters and average crystalline sizes of the synthesized ZnO NRs significantly changed as the growth temperature was increased. The obtained ZnO NRs' intensity along the (002) diffraction peak rose as the growth temperature increased, and the peak's hexagonal wurtzite plane orientation was preferred by the majority of ZnO NRs. The absorption edge changed toward longer wavelengths as growth temperature increased.

REFERENCES

1-V.R. Shinde, C.D. Lokhande, R.S. Mane, S.-H. Han, “Hydrophobic and textured ZnO films deposited by chemical bath deposition: annealing effect”, Appl. Surf. Sci. 245 (2005) 407–413.

2- O. Lupan, L. Chow, G. Chai, B. Roldan, A. Naitabdi, A. Schulte, H. Heinrich, “Nano fabrication and characterization of ZnO nanorod arrays and branched microrods by aqueous solution route and rapid thermal processing”, Mater. Sci. Eng. B Solid-State Mater. Adv. Technol. 145 (2007) 57–66.

3- A. Gimenez, “ZnO-Paper Based Photoconductive UV Sensor”, J. Phys. Vol. 2 (2010) 282–287.

4-S.K. Jha, O. Kutsay, I. Bello, S.T. Lee, “ZnO nanorod based low turn-on voltage LEDs with wide electroluminescence spectra”, J. Lumin. 133 (2013) 222–225.

5- Z.L. Wang, “ZnO nanowire and nanobelt platform for nanotechnology”, Mater. Sci. Eng. R Reports. 64 (2009) 33–71.

6- S. Desgreniers, “High-density phases of ZnO: Structural and compressive parameters”, Phys. Rev. B. 58 (1998) 14102–14105.

7- Z.L. Wang, “Nanostructures of zinc oxide, Mater”. Today. 7 (2004) 26–33.

8- S.S. Alias and A.A. Mohamad, “Synthesis of Zinc Oxide by Sol-gel method for Photoelectro-chemical Cells”, Springer Science + Business Media, (2014) 978981456074.

9-B.Y. Xia, P. Yang, Y. Sun, Y. Wu, B. Mayers, B. Gates, Y. Yin, F. Kim, H. Yan, “One-Dimensional Nanostructures: Synthesis, Characterization, and Applications”, Adv. Mater. (15) (2003) 353.

10-C.D. Lokwhande, “Chemical Deposition of Metal Chalcogenide Thin Films”, Mater. Chem. Phys. 27 (1991) 1–43.

11-R.S. Mane, C.D. Lokhande, “Chemical deposition method for metal chalcogenide thin films”, Mater. Chem. Phys. 65 (2000) 1–31.

12-A. F. Abdulrahman, N.M. Abd-Alghafour, Synthesis and characterization of ZnO nanoflowers by using simple spray pyrolysis technique, Solid-State Electronics, Volume 189, 2022, 108225,

13-H. M. Pathan and C. D. Lokhande, “Deposition of metal chalcogenide thin films by successive ionic layer adsorption and reaction (SILAR) Method”, Bull. Mater. Sci., 27(2) (2004) 85.

14-G. Sasikala, P. Thilakan,C. Subramanian, “Modification in the chemical bath deposition apparatus, growth and characterization of CdS semiconducting thin films for photovoltaic applications”, Solar Energy Materials and Solar Cells, 62 (2000) 275-293.

15-A. Sholehah, A. H. Yuwono, N. R. Poespawati , Ad. Trenggono , F. Maulidiah, “High Coverage ZnO Nanorods on ITO Susbtrates via Modified Chemical Bath Deposition (CBD) Method at Low Temperature”, Advanced Materials Research, 789 (2013) 151-156.

16-T. Lee, H. Ryu, W.-J. Lee, “Fast vertical growth of ZnO nanorods using a modified chemical bath deposition”, J. Alloys Compd. 597 (2014) 85–90.

17-A. F. Abdulrahman, S. M. Ahmed, S. M. Hamad, A. A. Barzinjy “Effect of Growth Temperature on Morphological, Structural, and Optical Properties of ZnO Nanorods Using Modified Chemical Bath Deposition Method”, Journal of Electronic Materials, 50, 1482–1495 (2021).

18-A. F. Abdulrahman, NM Abd-Alghafour, S. M Ahmed, “Optimization and characterization of SILAR synthesized ZnO nanorods for UV photodetector sensor”, Sensors and Actuators A: Physical, Vol. 323 (1), 112656, 2021.

19-Ahmed F. Abdulrahman, S. Mohammed Ahmed, A. Abdullah Barzinjy, S. Mustafa Hamad, Naser Mahmoud Ahmed, Munirah Abullah Almessiere, “Growth and Characterization of High-Quality UV Photodetectors Based ZnO Nanorods Using Traditional and Modified Chemical Bath Deposition Methods”, Nanomaterials, Vol. 11 (3), 677, 2021.

20-Ahmed F. Abdulrahman, “The Influence of Various Reactants in the Growth Solution on the Morphological and Structural Properties of ZnO Nanorods”, Passer Journal, Vol. 2 (2), 69-75, 2020.

21-Ercan Karak, and Hakan Çolak, Effect of substrate temperature on the structural properties of ZnO nanorods, Energy 141 (2017) 50-55.

22-F. Zahedi, R.S. Dariani, and S.M. Rozati, Effect of substrate temperature on the properties of ZnO thin films prepared by spray pyrolysis, Materials Science in Semiconductor Processing 16 (2013) 245–249.

23-Ishaq Musa, Naser Qamhieh, and Saleh Thaker Mahmoud, Synthesis and length dependent photoluminescence property of zinc oxide nanorods, Results in Physics 7 (2017) 3552–3556.

24-K. Salim and M. N. Amroun, Study of the Effects of Annealing Temperature on theProperties of ZnO Thin Films Grown by Spray PyrolysisTechnique for Photovoltaic Applications, Int. J. Thin. Film. Sci. Tec. 11, No. 1, 19-28 (2022).

25-Ahmed F. Abdulrahman “The effect of numerous substrate-inclined angles on the characteristic properties of ZnO nanorods for UV photodetectors applications”, Journal of Materials Science: Materials in Electronics, Vol.31 (17), 14357-14374, 2020.

26-Karam, S.T.; Abdulrahman, A.F. Green Synthesis and Characterization of ZnO Nanoparticles by Using Thyme Plant Leaf Extract. *Photonics* 2022, *9*, 594. https://doi.org/10.3390/photonics9080594.

27-Abdulqudos, A., Abdulrahman, A. F. (2022). 'Biosynthesis and Characterization of ZnO Nanoparticles by using Leaf Extraction of Allium Calocephalum Wendelbow Plant', Passer Journal of Basic and Applied Sciences, 4(2), pp. 113-126. doi: 10.24271/psr.2022.343112.1136.

28-W. B. Mi, and H. L. Bai, Microstructure, magnetic, and optical properties of sputtered Mn-doped ZnO films with high-temperature ferromagnetism, Journal of Applied Physics 101, 023904 (2007).

29-Abdulrahman AF, Ahmed SM, Ahmed NM, Almessiere MA. Enhancement of ZnO Nanorods Properties Using Modified Chemical Bath Deposition Method: Effect of Precursor Concentration. *Crystals*. 2020; 10(5):386. https://doi.org/10.3390/cryst10050386

30-Hongmei Zhong, Jinbing Wang, Xiaoshuang Chena), Zhifeng Li, Wenlan Xu, and Wei Lu, Effect of Mn+ ion implantation on the Raman spectra of ZnO, Journal of Applied Physics 99, 103905 (2006); https://doi.org/10.1063/1.2197262

31-Erki Kärber, Taavi Raadik, Tatjana Dedova, Jüri Krustok, Arvo Mere, Valdek Mikli and Malle Krunks, Photoluminescence of spray pyrolysis deposited ZnO nanorods, Nanoscale Research Letters 2011, 6:359.

32-Rusli NI, Tanikawa M, Mahmood MR, Yasui K, Hashim AM. Growth of High-Density Zinc Oxide Nanorods on Porous Silicon by Thermal Evaporation. *Materials*. 2012; 5(12):2817-2832. https://doi.org/10.3390/ma5122817.

33-Wai Kian Tan, Khairunisak Abdul Razak, Zainovia Lockman, Go Kawamura, Hiroyuki Muto, Atsunori Matsuda, Synthesis of ZnO nanorod–nanosheet composite via facile hydrothermal method and their photocatalytic activities under visible-light irradiation, Journal of Solid-State Chemistry, Volume 211, 2014, 146-153.